Available online at ScienceDirect

Nuclear Engineering and Technology

journal homepage: www.elsevier.com/locate/net

Original Article

Effective Thermal Conductivity and Diffusivity of Containment Wall for Nuclear Power Plant OPR1000

Hyung Gyun Noh [a], *Jong Hwi Lee* [b], *Hie Chan Kang* [b,*], *and Hyun Sun Park* [a]

[a] *Division of Advanced Nuclear Engineering (DANE), Pohang University of Science and Technology (POSTECH), 30, Jigok-ro 127 beon-gil, Nam-gu, Pohang-si, Gyeongsangbuk-do 37673, Republic of Korea*

[b] *Mechanical Engineering Division, Kunsan National University (KNU), 558, Daehak-ro, Gunsan-si, Jeollabuk-do 54150, Republic of Korea*

ARTICLE INFO

Article history:
Received 30 May 2016
Received in revised form
14 August 2016
Accepted 15 October 2016
Available online 9 February 2017

Keywords:
Containment Wall
Thermal Conductivity
Thermal Diffusivity
Reinforced Concrete
Severe Accident

ABSTRACT

The goal of this study is to evaluate the effective thermal conductivity and diffusivity of containment walls as heat sinks or passive cooling systems during nuclear power plant (NPP) accidents. Containment walls consist of steel reinforced concrete, steel liners, and tendons, and provide the main thermal resistance of the heat sinks, which varies with the volume fraction and geometric alignment of the rebar and tendons, as well as the temperature and chemical composition. The target geometry for the containment walls of this work is the standard Korean NPP OPR1000. Sample tests and numerical simulations are conducted to verify the correlations for models with different densities of concrete, volume fractions, and alignments of steel. Estimation of the effective thermal conductivity and diffusivity of the containment wall models is proposed. The Maxwell model and modified Rayleigh volume fraction model employed in the present work predict the experiment and finite volume method (FVM) results well. The effective thermal conductivity and diffusivity of the containment walls are summarized as functions of density, temperature, and the volume fraction of steel for the analysis of the NPP accidents.

1. Introduction

After the Fukushima accident, accurate analysis of the pressure and temperature inside the containment is a very important issue. Removal of the internal heat is absolutely vital to mitigate accident progression, which may compromise the integrity of the containment and release radioactive material into the environment. Recently, in containment analysis, a containment building including deformed bars and tendons was considered as a passive heat sink source [1]. Thus, investigation of the effective thermal conductivity and diffusivity is needed for more accurate analysis in the containment wall.

The main objective of this study is to propose an effective thermal conductivity model for containment walls for thermal hydraulic codes such as Containment Analysis Package (CAP), MARS, and CONTAIN. Containment walls are composite structures that consist of concrete, rebar, steel liners, and

* *Corresponding author.*
E-mail address: hckang@kunsan.ac.kr (H.C. Kang).
http://dx.doi.org/10.1016/j.net.2016.10.010

tendons; the geometries of these materials vary in nuclear power plants (NPPs). We focus on NPP model OPR1000, which is adopted at 12 Korean sites including the Shin-Wolsong Units 1 and 2 located in Gyeongju, as our test case. For composite materials, many effective thermal conductivity models are presented. In this paper, several models are applied to evaluate the effective thermal conductivity of reinforced concrete, which is mainly composed of concrete and steel.

Maxwell [2] suggested an analytical model for predicting the representative or effective thermal conductivity of the composite materials. The model predicts diluted random-sized spheres in a matrix for volume fractions under 25%. The Rayleigh sphere model [3] contains spherical particles packed regularly in a solid. This model includes thermal interaction among the particles to enhance Maxwell's model. The Rayleigh cylinder model [4] provides analytical correlations for cylindrical particles embedded in a solid. This model can estimate the directional effective thermal conductivity when the cylindrical particles are located parallel (x) and perpendicular (y) to the heat transfer direction (x) [4]. The model is valid when the cylinder rods are totally penetrated in a solid. The Rayleigh volume fraction model, adapted from the Rayleigh cylinder model, is proposed to consider the cylindrical shapes of the rebar and tendons in the present work.

The containment walls include steel rebar and cylindrical tendons with different orientations and volume fractions. The thermal properties of the reinforced concrete are functions of density, temperature, chemical composition, volume fraction of steel, etc. Effective thermal conductivity tests were conducted on concrete of different compositions, and numerical simulations were conducted to compare the models with up to 25% volume fraction of steel. Equations for evaluating the effective thermal conductivity and diffusivity of containment walls under crisis conditions are summarized.

2. Models and verification method

2.1. Containment wall of OPR1000

The containment building of the OPR1000 is a type of pre-stressed concrete containment vessel. Its inner diameter is 43.9 m and its height is 66.8 m. Fig. 1 shows the containment wall structure for the OPR1000, which consists of concrete, tendons, a steel liner, and deformed rebar. The rebar has ribs, and the steel and concrete are fused in the nodes. The steel liner acts as a leak-tightness. Tendons made of twisted steel wire add tensile force. The specifications of the materials are regulated: deformed bar (ASTM A615 Grade 60), tendons (ASTM A416 Grade 270), and steel liner (SA516 Grade 60). The typical thickness of the containment wall is 1.2 m. The rebar ranges from 25 mm to 50 mm in diameter, and the diameter of the tendons is on the order of 250 mm. The containment wall of the OPR1000 contains about 11% steel by volume.

2.2. Effective thermal conductivity models for simple geometry

The models proposed for estimating the effective thermal conductivity of the composite materials are summarized by the following equations where: k_{eff} = effective thermal conductivity in reinforced concrete (W/m·K), k_c = concrete thermal conductivity (W/m·K), k_s = steel thermal conductivity (W/m·K), ϕ = volume fraction of steel, ϕ_i = volume fraction of steel in i direction, β_i = i-axis ratio in total steel volume, ρ_c = concrete density (kg/m^3), ρ_s = steel density (kg/m^3), ρ_{mix} = mixture density (kg/m^3), $C_{p,s}$ = steel heat capacity (J/kg·K), $C_{p,c}$ = concrete heat capacity (J/kg·K), $C_{p,mix}$ = mixture heat capacity (J/kg·K), and α_{eff} = effective thermal diffusivity in reinforced concrete (m^2/s).

The Maxwell model [2] considers composite materials as spherical particles spread thinly over a continuous matrix. The Rayleigh sphere model [3] presents uniformly distributed spherical particles, and accounts for interactions among them. The Rayleigh cylinder model [4] updates the effective thermal conductivity model to include cylindrical particles as well. This model accounts for the heat transfer direction and orientation of the particles. Tendons and rebar rods are distributed in three-dimensional directions, as shown in Fig. 1. The Rayleigh cylinder model is modified from the so-called Rayleigh volume fraction model in the present work to consider the directional contribution. In this new model, the amounts of the volume fractions are multiplied by their effective thermal conductivities to yield their contributions along the parallel (x) and perpendicular (y) directions:

Maxwell [2]:

$$\frac{k_{eff}}{k_c} = 1 + \frac{3\phi}{\left(\frac{k_s+2k_c}{k_s-k_c}\right) - \phi}, \phi \le 0.25 \quad (1)$$

Rayleigh sphere [3]:

$$\frac{k_{eff}}{k_c} = 1 + \frac{3\phi}{\left(\frac{k_s-2k_c}{k_s-k_c}\right) - \phi + 1.569\left(\frac{k_s-k_c}{3k_s-4k_c}\right)\phi^{\frac{10}{3}} + \ldots} \quad (2)$$

Rayleigh cylinder-x [4]:

$$\frac{k_{eff}}{k_c} = 1 + \frac{k_s - k_c}{k_c}\phi \quad (3)$$

Rayleigh cylinder-y [4]:

$$\frac{k_{eff}}{k_c} = 1 + \frac{2\phi}{\left(\frac{k_s+k_c}{k_s-k_c}\right) - \phi + \left(\frac{k_s-k_c}{k_s+k_c}\right)(0.30584\phi^4 + 0.013363\phi^8 + \ldots)} \quad (4)$$

Rayleigh volume fraction:

$$k_{eff} = \frac{\phi_x}{\phi}k_{eff,\ Rayleigh\ \ cylinder-x} + \frac{\phi_y}{\phi}k_{eff,\ Rayleigh\ \ cylinder-y} \quad (5)$$

2.3. Experiment

Concrete is a composite of cement, gravel, and sand; its thermal properties are functions of the fractions of these materials. The present work measured the density and thermal conductivity of specimens with dimensions of 100 mm × 100 mm × 20 mm. The ratio of cement to gravel to sand was 5:4:4. The thermal conductivity was measured using the steady-state thermal resistance method according to regulation KS L ISO 8302 with a TLP-300 (Taurus Instruments, Munchen, Germany). The accuracy of the measurements was ± 0.05 W/m·K. The concrete powder used to form the specimens was sifted through a 10 mm sieve. The chemical compositions of the samples were

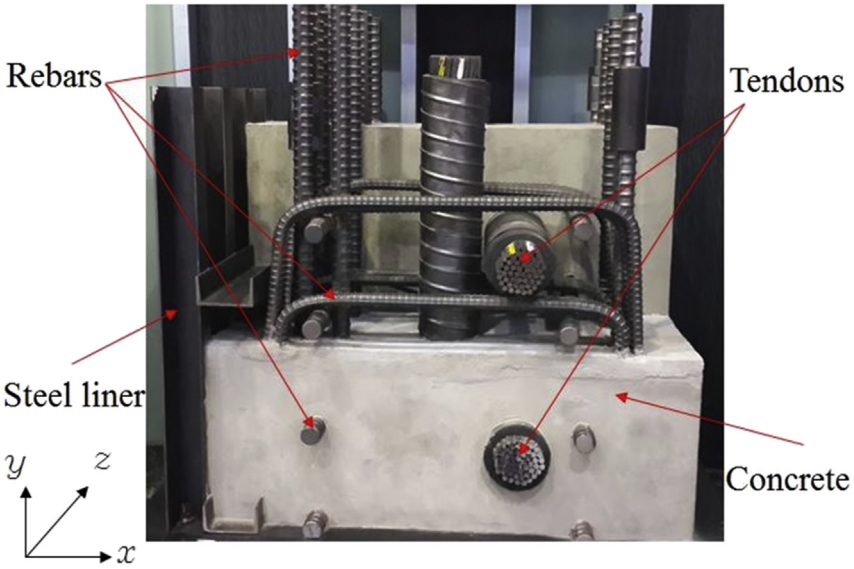

Fig. 1 – Structure of containment wall of standard Korean nuclear power plant OPR1000.

Table 1 – Chemical compositions of concretes used in nuclear power plants (NPPs) (wt%) [5].

Composition	Siliceous	Limestone	Hanbit Units 3 & 4	Present test
SiO_2	69.7	7.0	55.7	41.3
CaO	13.7	42.4	15.8	27.5
Al_2O_3	4.0	1.9	10.3	8.0
K_2O	1.4	0.4	2.9	2.0
Na_2O	0.7	0.0	2.0	1.0
$MgO/MnO/TiO_2$	1.5	7.4	1.6	2.3
Fe_2O_3	1.0	0.8	2.6	4.9
Cr_2O_3	0.0	0.0	0.02	0.0
H_2O	6.9	6.9	7.2	12.9
CO_2	1.0	33.2	2.8	–
P_2O_5	–	–	–	0.1

examined with an X-ray fluorescence spectrometer (Shimadzu XRF-1700). The results are shown in Table 1.

2.4. *Numerical simulations*

The finite volume method (FVM) was used to investigate the effective thermal conductivity of the OPR1000 containment wall. The rebar pattern was roughly a repeating 1.2 m × 1.2 m area, so this unit was used for the calculations in the present work. The rebar and tendons, as shown in Fig. 2, were 50 mm and 250 mm in diameter, respectively. The rebar and tendons were simplified as octagonal bars, and the rebar was considered to be welded at the joints. The thermal resistance of air inside the tendons was ignored. Numerical simulations were conducted using ANSYS CFX16 in the steady-state condition. A 1.7 million-unit tetra grid was used. For the convergence conditions, the sum of the residuals was less than 10^{-6}, and the energy balances were over 99.9%. Constant temperature conditions of 417 K and 288 K were applied to the inside and outside surfaces of the wall, respectively. Periodic conditions were applied to the repeated side surfaces. The locations of the periodic conditions were z = 0, 1.2 m, and y = 0, 1.2 m, respectively. The thermal conductivities used for the concrete and steel in the numerical simulations were constant as 1.6 W/m·K and 47 W/m·K, respectively. Numerical simulations of heat conduction confirmed the case for bare concrete prior to the present work. The volume fraction of the steel varied with the diameter of the rebar and tendons by up to 25%.

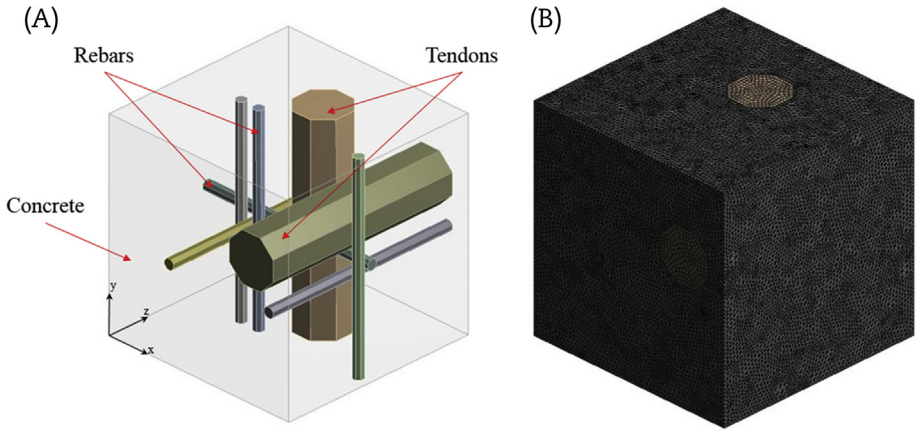

Fig. 2 – Numerical domain and grid in containment wall of OPR1000. (A) Calculation domain. (B) Numerical grid.

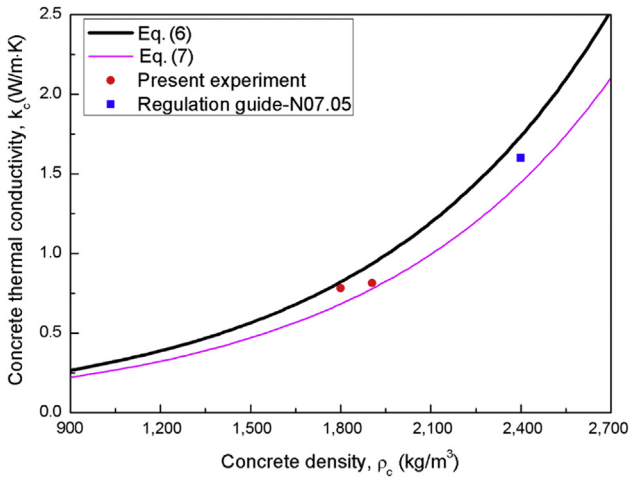

Fig. 3 – Concrete thermal conductivity over density.

3. Results and discussion

3.1. *Thermal properties of concrete*

The concrete matrix of the containment wall contains chemicals such as calcium monoxide, silicon dioxide, aluminum oxide, etc. Types of concrete include siliceous concrete and limestone concrete. Shin et al [5] proposed empirical correlations for specific concrete for elevated temperatures for the Hanbit NPP Units 3 and 4. The general concrete type of Korean NPPs is similar to the siliceous concrete used in Hanbit Units 3 and 4. Chemical compositions for concrete types are listed in Table 1.

The thermal conductivity of concrete is a function of temperature, chemical composition, curing conditions, and density. Thermal conductivity can be expressed as a function of density at normal temperatures as in the following equations [6]. The coefficients for these equations were influenced by the curing conditions (air-dried or oven-dried).

$$k_c = 0.0865e^{0.00125\rho_c} \text{ for air drying} \quad (6)$$

$$k_c = 0.0720e^{0.00125\rho_c} \text{ for oven drying} \quad (7)$$

The thermal conductivities of the present specimens were estimated on account of their low average density (1852 kg/m^3) compared to the value listed in the regulation guide (2,400 kg/m^3) (Fig. 3). The experimental values for conductivity were lower than the 1.6 W/m·K value in the regulation guide [1] and varied with density. However, the present experimental data and the value in the regulation guide are located between the values delivered in Eqs. (6) and (7). Therefore, the thermal conductivity of the concrete is more a function of its density than of its chemical composition.

The thermal conductivity of concrete is a function of temperature. Suggested correlations for thermal conductivity depending on concrete type and temperature are given in the following equations [7].

Siliceous:

$$\begin{aligned} k_c &= 1.5 - 0.000625T, (20^\circ\text{C} \le T \le 800^\circ\text{C}) \\ k_c &= 1.0, (T > 800^\circ\text{C}) \end{aligned} \quad (8)$$

Limestone:

$$\begin{aligned} k_c &= 1.355, (20^\circ\text{C} \le T \le 293^\circ\text{C}) \\ k_c &= 1.7162 - 0.001241T, (T > 293^\circ\text{C}) \end{aligned} \quad (9)$$

Hanbit Units 3 and 4:

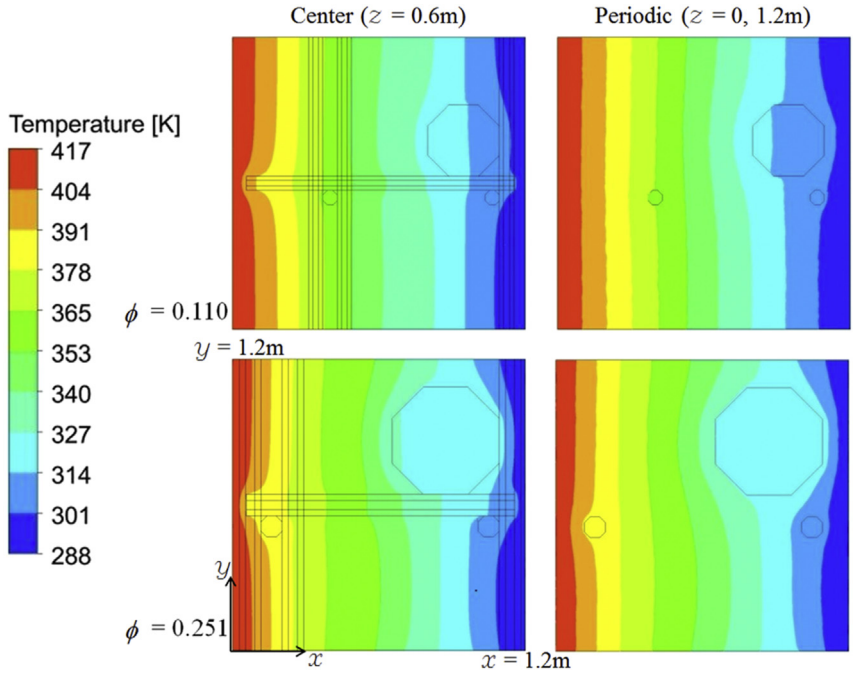

Fig. 4 – Temperature distributions in center and periodic cross sections of containment wall for volume fractions ϕ = 0.110 and ϕ = 0.251.

$$k_c = 2.24266 - 0.00256908\,T + 1.36469\,E - 6T^2, (20^\circ C \le T \le 900^\circ C) \quad (10)$$

3.2. Thermal properties of containment wall

The effective thermal conductivity versus volume fraction of steel was determined. The overall temperature distribution shifted to the right as the volume fraction increased (Fig. 4). The size of the tendons played an important role in the temperature gradient.

The values of the effective thermal conductivity models were compared with results from FVM and the experiments conducted to obtain the effective thermal conductivity of the reinforced concrete as a volume fraction. A graph of the results is shown in Fig. 5. Nondimensional effective thermal conductivity is used for comparison in identical conditions due to the difference of concrete conductivity. Kanbur et al [8] determined the thermal conductivity of the reinforced concrete for different volume fractions. Diameters of reinforcement bars of 10 mm and 12 mm were used in their experiment. Model size was 500 mm × 500 mm × 100 mm and length of reinforcement bars was 90 mm. The rebar was positioned in the heat transfer direction. The smallest difference from the experimental results is shown in the Rayleigh cylinder x model on account of its direction. The discrepancies between the Rayleigh cylinder x model and Kanbur et al's [8] experimental data are about 10.2% and 10.3% individually. Their data presented a lower conductivity estimation than did the Rayleigh cylinder x model, because the reinforced bars were not fully penetrated in the concrete. Zhao et al [9] made reinforced concrete with the rebar orthogonal to the heat transfer direction. The steel bars were located in a horizontal one-way direction for the 1.7% and 2.7% volume fractions. By contrast, the steel bars were arranged in both directions for

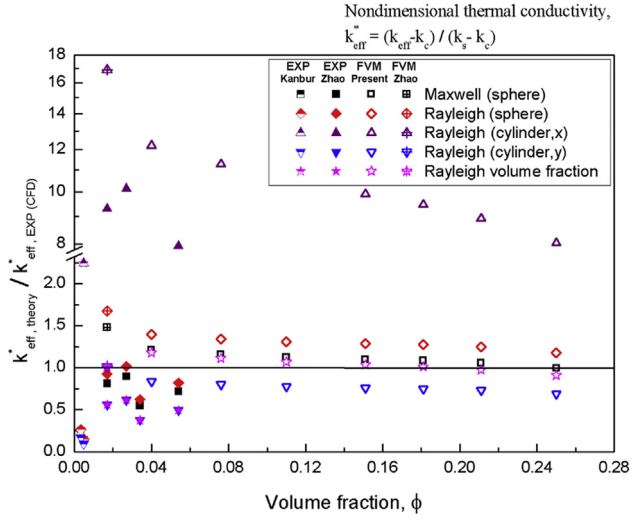

Fig. 5 – Comparisons of effective thermal conductivity models, experimental data, and finite volume method (FVM) results for the reinforced concretes with various volume fractions at the ambient temperature.

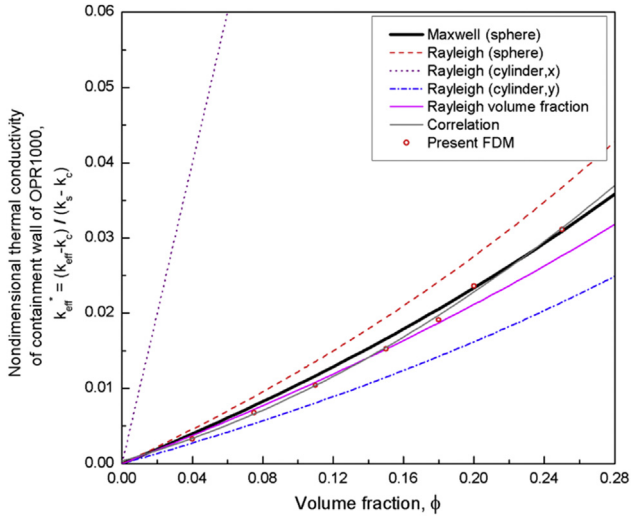

Fig. 6 – Nondimensional thermal conductivity versus volume fraction of OPR1000 containment wall.

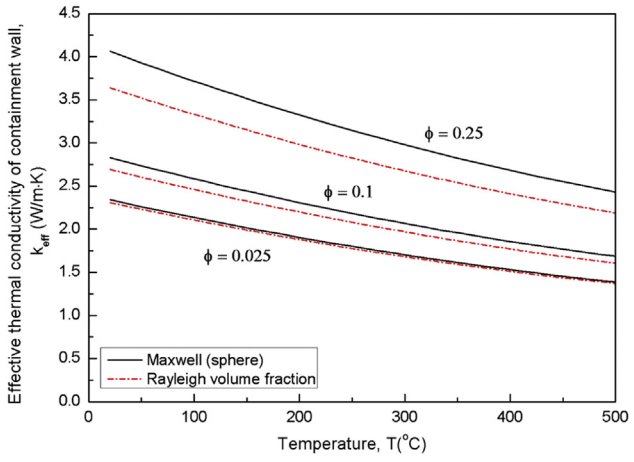

Fig. 7 – Effective thermal conductivity of containment wall over temperature ($20^\circ C \le T \le 900^\circ C$).

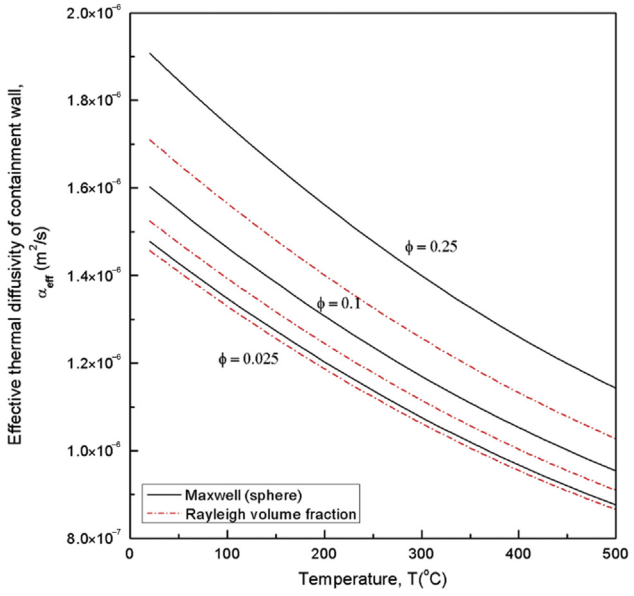

Fig. 8 – Effective thermal diffusivity of containment wall versus temperature ($20^\circ C \le T \le 900^\circ C$).

Table 2 – Thermal properties of containment wall and their correlations.

Thermal Properties	Units	Correlations		Remarks
Density	kg/m^3	$\rho_{mix} = \rho_s\phi + \rho_c(1-\phi)$	(12)	
Heat capacity	J/kg·K	$C_{p,mix} = C_{p,s}\phi\frac{\rho_s}{\rho_{mix}} + C_{p,c}(1-\phi)\frac{\rho_c}{\rho_{mix}}$	(13)	
Thermal conductivity	W/m·K	$k_{eff} = \frac{\phi_x}{\phi}k_{\text{eff, Rayleigh cylinder-x}} + \frac{\phi_y}{\phi}k_{\text{eff, Rayleigh cylinder-y}}$	(14)	
Thermal diffusivity	m^2/s	$\alpha_{eff} = \frac{k_{eff}}{\rho_{mix}C_{p,mix}}$	(15)	
Concrete density	kg/m^3	$\rho_c = 2259.62 - 0.39802\ T + 0.000189575\ T^2 (20^\circ C \le T \le 1100^\circ C)$	(16)	Shin et al [5] (Hanbit Units 3 & 4)
Steel density	kg/m^3	$\rho_s = 7850$	(17)	Korea Institute of Nuclear Safety [1]
Concrete heat capacity	J/kg·K	$C_{p,c} = 654$	(18)	
Steel heat capacity	J/kg·K	$C_{p,s} = 503$	(19)	
Steel thermal conductivity	W/m·K	$k_s = 54 - 0.0333\,T, (20^\circ C \le T \le 800^\circ C)$ $k_s = 27.3, (800 < T \le 1200^\circ C)$	(20)	Phan et al [10]

the 3.4% and 5.4% volume fractions. Specimen size was 300 mm × 300 mm × 50 mm and the diameter of the steel bars was 8 mm. Most models are well matched with Zhao et al's data, except for the Rayleigh cylinder x model. The range of the standard deviation is 3.25–6.74% between the models and the experimental data. For this reason, a numerical simulation was conducted under the same conditions as those used in Zhao et al's [9] experiment, with a 0.017 volume fraction, as shown in Fig. 5. The discrepancy between the Rayleigh volume fraction model and the numerical simulation was about 1.55%. Therefore, the difficulty of model comparison is due to the low volume fraction range of Zhao et al's [9] experiment.

The Rayleigh volume fraction model was the best predictor among the models for the OPR1000 containment wall under the 0.2 volume fraction because it considered the heat transfer of the steel bars in three directions (Fig. 6). The difference between the Rayleigh volume fraction model and the numerical simulation was about 4.2%. Maxwell's [2] model showed higher values than Rayleigh's volume fraction model and agreed well with the FVM results for volume fractions over 0.2. By contrast, the Rayleigh cylinder-x model greatly overestimated the results because it assumed that the steel penetrated a bulk solid. Certainly, the volume fraction of the steel has significant effects on the effective thermal conductivity of the containment wall. The empirical correlation for FVM with volume fractions at 15°C is expressed in the following equation:

$$k^*_{eff} = 0.2176\,\phi^2 + 0.06711\,\phi + 0.0001742, (0 < \phi < 0.25) \quad (11)$$

In cases of severe accidents, the temperature of the containment structure will change. Therefore, effective thermal conductivity over a range of temperatures must be proposed in order to use the containment wall as a heat sink. The thermal conductivities of concrete and steel vary with temperature. The effective thermal conductivity of the Rayleigh volume fraction model over a range of temperatures is suggested in Fig. 7. The containment wall of the NPP OPR1000 includes about 11% steel. The effective thermal conductivity of the containment wall decreases as temperature increases owing to properties of the concrete and steel.

Thermal diffusivity is expressed as conduction heat divided by storage heat and is an important property for transient heat transfer. The effective thermal diffusivity of the containment wall was calculated as a function of the temperature and the volume fraction of steel (Fig. 8). It decreased as the temperature and volume fraction of steel increased. Correlations for the effective thermal diffusivity are described in Table 2.

3.3. *Limitations and comments*

The effect of the steel liner is not considered in this work because it is very thin compared to the containment wall; the authors recommend considering its thermal resistance separately. The thermal properties of reinforced concrete are summarized in Table 2. The applicable range of the temperature is specified, and the recommended volume fraction of the steel is < 25%.

4. Conclusion

In the present work, the effective thermal properties of the containment wall were investigated as critical properties for heat removal in nuclear accidents. Theoretical models were applied to the standard Korean NPP OPR1000, and results were compared with FVM results and experimental data. The Rayleigh volume fraction model (modified from the Rayleigh cylinder model) and the Maxwell [2] model, with 4.2% and 5.8% of the standard deviations, respectively, are recommended for the containment wall up to 25% of volume fraction. The effective thermal conductivity and thermal diffusivity correlations as functions of the temperature and volume fraction of the steel are provided for analyses of NPP accidents. Using codes such as MARS, CAP, and CONTAIN, the present results can improve the accuracy of analyses when the containment building functions as a heat sink or passive cooling system during a NPP accident. The present work will be valuable for the investigation of the effective thermal conductivities of the general containment wall of the OPR1000.

Conflicts of interest

All authors have no conflicts of interest to declare.

Acknowledgments

This work was supported by a National Research Foundation of Korea (NRF-2015M2B2A9031638) grant funded by the Korean government.

Nomenclature

k_{eff}	Effective thermal conductivity in reinforced concrete (W/m·K)
k_c	Concrete thermal conductivity (W/m·K)
k_s	Steel thermal conductivity (W/m·K)
ϕ	Volume fraction of steel
ϕ_i	Volume fraction of steel in i direction
β_i	i-axis ratio in total steel volume
ρ_c	Concrete density (kg/m^3)
ρ_s	Steel density (kg/m^3)
ρ_{mix}	Mixture density (kg/m^3)
$C_{p,s}$	Steel heat capacity (J/kg·K)
$C_{p,c}$	Concrete heat capacity (J/kg·K)
$C_{p,mix}$	Mixture heat capacity (J/kg·K)
α_{eff}	Effective thermal diffusivity in reinforced concrete (m^2/s)

REFERENCES

[1] Korea Institute of Nuclear Safety, Containment System of Containment Design Analysis, Regulation Guide, 2015.

[2] J.C. Maxwell, 1831–1879: A Treatise on Electricity and Magnetism, Clarendon Press, Oxford, 1904.

[3] J. Strutt (Lord Rayleigh), On the Influence of Obstacles Arranged in Rectangular Order upon the Properties of a Medium, Philosophical Magazine, 1892.

[4] K. Pietrak, S. Tomasz Wisniewski, A review of models for effective thermal conductivity of composite materials, J. Power Technol. 95 (2015) 14–24.

[5] K.Y. Shin, S.B. Kim, J.H. Kim, M. Chung, P.S. Jung, Thermo-physical properties and transient heat transfer of concrete at elevated temperatures, Nucl. Eng. Des. 212 (2002) 223–241.

[6] K. Cavanaugh, Guide to Thermal Properties of Concrete and Masonry Systems, American Concrete Institute, 2002.

[7] U.S.NRC, A Compilation of Elevated Temperature Concrete Material Property Data and Information for Use in Assessments of Nuclear Power Plant Reinforced Concrete Structures, NUREG/CR-7031, 2009.

[8] B.B. Kanbur, S.O. Atayilmaz, H. Demir, A. Koca, Z. Gemici, Investigating the thermal conductivity of different concrete and reinforced concrete models with numerical and experimental methods, Recent Adv. Mech. Eng. Appl. (2013) 95–101.

[9] S. Zhao, S. Yang, X. Feng, M. Lu, Study on thermal conductivity of reinforced concrete plate, Applied Mechanics and Materials 438–439 (2013) 321–328.

[10] L.T. Phan, T.P. McAllister, J.L. Gross, M.J. Hurley, Best Practice Guidelines for Structural Fire Resistance Design of Concrete and Steel Buildings, NIST Technical Note 1681, 2010.